Reduced Critical Current Anisotropy and Improved Critical Current Performance in a Combined Pinning Landscape Created by Proton and Silver Irradiation

Arya A. Soman, Stuart C. Wimbush, *Senior Member, IEEE*, Nicholas J. Long, Martin W. Rupich, Christian Notthoff, Patrick Kluth, Jerome Leveneur, John Kennedy, and Nicholas M. Strickland

***Abstract*—Particle irradiation using light ions and heavy ions is found to be an effective method to introduce flux-pinning centers into REBCO films and coated conductors. The degree of enhanced critical current at various conditions depends upon the size, morphology, and orientation of ion tracks. Proton irradiation to the optimised fluence results in greater isotropic enhancement at lower temperatures, the enhancement decreases as temperature increases. Silver ion irradiation on the other hand gives a greater enhancement at higher temperature but limited to particular angular ranges. We compare the results of these two types of irradiation and then produce a mixed pinning landscape with a combination of the two. We find a nearly isotropic enhancement in I_c at lower temperatures and an enhancement about the *c*-axis direction, similar but broader than silver irradiation alone, at higher temperatures.**

***Index Terms*—REBCO coated conductors, ion irradiation, critical current anisotropy, vortex pinning, intrinsic pinning, composite pinning landscape, maximum entropy.**

I. Introduction

IN RECENT years, high temperature superconducting (HTS) wires based on $REBa_2Cu_3O_7$ (REBCO, RE: rare earth elements) have been employed in many devices and technologies contributing to high energy efficiency and low carbon energy [1]. Achieving high critical current density and reducing the magnetic field anisotropy of critical current are current research goals [2], [3]. Pinning flux lines through engineered nano-scale defects has been extensively studied [4], [5]. Particle irradiation is one effective way to introduce additional pinning centers in a controlled way and with minimal disruption to the pre-existing defect landscape. Irradiation with protons [6], [7] and with heavy ions [8], [9] such as silver [10] can give quite distinct changes to the material and therefore have different effects on pinning over different conditions of temperature, magnetic field and field orientation.

Proton irradiation creates defects which act as effective pinning centers especially at lower temperature, high magnetic field. Transmission electron microscopy (TEM) has shown that MeV-range protons produce point-like defects [7] and would therefore be likely to produce a nearly isotropic I_c enhancement. Silver irradiation in the range 75 MeV–100 MeV is found to be better than proton irradiation in creating perpendicular-field I_c enhancement. TEM studies have shown that irradiation in this energy range produces discontinuous columnar tracks [10], [11], [12]. At low temperatures these tracks have also been found to give strong isotropic enhancement to pinning through cooperative pinning with intrinsic pins and point defects, however, this isotropic lift is lost at higher temperatures [12]. Here, we directly compare irradiation by 1.2 MeV protons and 125 MeV silver ions each individually and then in a combined irradiation.

II. Materials and Experimental Details

The tape under investigation was obtained from the AMSC production line prior to lamination [13]. It has a 1.4 μm thick HTS layer with nominal composition $YBa_2Cu_3O_7 + 0.25\,Dy_2O_3$ deposited by metal-organic deposition and is capped with a 1 μm thick silver layer. The material is consistent in its properties along the length and already engineered for high performance at low temperature and high field.

Samples for irradiation were patterned using a nanosecond pulsed laser to a bridge 5 mm long and 0.5 mm wide to facilitate uniform irradiation throughout the measurement area and to maintain the critical current within a convenient range. Irradiation with 125 MeV Ag ions was carried out at the ANU Heavy Ion Accelerator Facility (Australia) and 1.2 MeV proton irradiation was performed at the GNS Van de Graaff positive ion accelerator (New Zealand). Annealing was performed in a tube furnace under a flowing O_2 atmosphere at a temperature of 300 °C for 1 hour after silver irradiation and/or 200 °C annealing for 1 hour after proton irradiation. The lower temperature for proton irradiation avoided annealing out the smaller pinning defects

Manuscript received 13 November 2022; revised 15 January 2023 and 3 February 2023; accepted 7 February 2023. Date of publication 13 February 2023; date of current version 21 February 2023. This work was supported in part by the Royal Society of New Zealand under Marsden Fund Grant VUW1805. We acknowledge access to the Heavy-Ion Accelerator Facility funded under the National Collaborative Research Infrastructure Strategy (NCRIS), Australia. *(Corresponding author: Arya A. Soman.)*

Arya A. Soman, Stuart C. Wimbush, Nicholas J. Long, and Nicholas M. Strickland are with the Robinson Research Institute, Victoria University of Wellington, Lower Hutt 5010, New Zealand (e-mail: ar-ya.ambadiyilsoman@vuw.ac.nz).

Martin W. Rupich is with the American Superconductor Corporation, Ayer, MA 01432 USA.

Christian Notthoff and Patrick Kluth are with the Research School of Physics, Australian National University, Canberra, ACT 2601, Australia.

Jerome Leveneur and John Kennedy are with the GNS Science, Lower Hutt 5010, New Zealand.

Color versions of one or more figures in this article are available at https://doi.org/10.1109/TASC.2023.3244522.

Digital Object Identifier 10.1109/TASC.2023.3244522

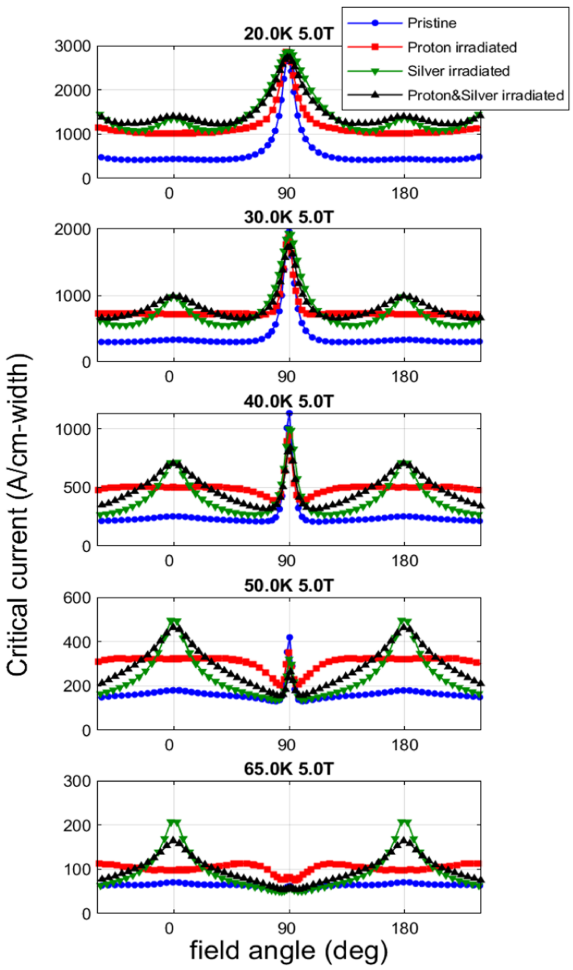

Fig. 1. Angle dependence of the critical current of the sample before irradiation and samples with proton, silver, and combined irradiation at temperature range of 20 K–65 K and magnetic field of 5 T.

created with this irradiation. The combined sample was annealed at both 300 °C (after silver irradiation) and at 200 °C (after proton irradiation). This treatment improves the critical current performance without annealing out the core defects created by proton and silver irradiation [14], [15]. The critical current was measured over a range of temperatures (20 K–77.5 K), magnetic fields up to 8 T and magnetic field angles on a SuperCurrent four-probe transport measurement system [16], [17] available at Robinson Research Institute, New Zealand.

III. Results and Discussion

A. Angle Dependence of Critical Current

The temperature dependences of the critical current $I_c(\theta)$ between 20 K and 65 K at magnetic field of 5 T are shown in Fig. 1. An unirradiated sample (pristine) and samples irradiated with individual ions (silver irradiated or proton irradiated) and combined sample (Proton+silver irradiated) are compared. Distinctly different angular features are seen to arise for the different types of pinning centres arising and there is also a clear trend of peak widths across the range of temperatures.

The pristine sample used in the current investigation has an I_c anisotropy that varies across this temperature range. At low temperatures it has a dominant and quite sharp *ab*-peak (90°) and a flat background across the *c*-axis. The *ab*-peak becomes sharper but relatively weaker going to higher temperatures until at 65 K it is barely seen leaving the I_c almost completely isotropic. The flat background represents the presence of isotropic pinning centers (point defects and nanoparticles) while the strong *ab*-peak arises from intrinsic pinning which diminishes with increasing temperature [18].

The proton irradiated sample using 1.2 MeV protons with fluence 1.3×10^{16} protons/cm^2 creates point defects [19], [20], [7] which give enhanced isotropic pinning over the entire temperature range. At 20 K, 5 T proton irradiation gives a factor 2.3 of *c*-axis I_c enhancement. Notably, the width of the *ab*-peak is not significantly affected by proton irradiation. As the temperature increases, the *c*-axis enhancement reduces reaching 1.38 at 65 K, 5 T. This is due to the point defects becoming less effective in pinning as temperature increased due to the increased coherence length of vortices [12], [20].

The introduction of columnar defects by 125 MeV silver irradiation to a fluence of 4×10^{11} ions/cm^2 results in a significant *c*-axis enhancement at all temperatures. Unlike proton irradiation, the *c*-axis enhancement is not reduced with increasing temperature, maintaining approximately a factor of 3 at all temperatures at 5 T from 20 K to 65 K. At low temperature the columnar defects also produce a quite isotropic enhancement [11] through broadening of the *ab* and *c*-axis peaks. However, at higher temperatures the enhancement is concentrated at the *c*-axis direction and at intermediate angles the enhancement of the $I_c^{\min}$ decreases with temperature to the point that there is a slight reduction in $I_c^{\min}$ value at 65 K relative to the pristine sample. The silver irradiation also results in significant broadening of the *ab*-peak at lower temperatures relative to either the pristine or the proton irradiated samples. However, from 40 K onwards, this broadening does not occur, and the width of the *ab*-peak is approximately unchanged with silver irradiation.

The sequential irradiation of silver ions followed by protons results in a combined pinning landscape with large number of point defects and linear tracks parallel to the *c*-axis. At lower temperatures of 20 K and 30 K, there is an overall benefit with the combination. The introduced point and columnar defects result in a broader *c*-axis peak, maintaining the same peak enhancement as silver irradiation as well as the same isotropic enhancement by proton irradiation. From 40 K onwards the point defects help in broadening the *c*-axis peak reducing the anisotropy relative to silver irradiation alone and maintaining higher enhancement in *c*-axis direction with silver irradiated tracks as well as a better enhancement of the angular minimum I_c, $I_c^{\min}$, than for silver irradiation alone.

Fig. 2(a) shows I_c along the *c*-axis for all the four different samples with increasing temperature. The *c*-axis peak strength is observed to be same for silver and combined irradiation at lower temperature, giving no benefit of addition of protons along with silver in bring up the 0° peak. However, the angular minimum I_c, the $I_c^{\min}$, dependence on temperature shown in Fig. 2b shows that $I_c^{\min}$is improved by the combination, a 13% increased value

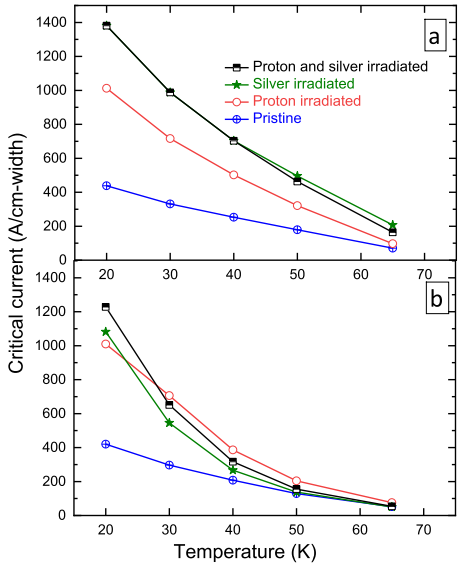

Fig. 2. Temperature dependences of the critical current in a 5 T magnetic field for (a) perpendicular field, and (b) the angular minimum, for the unirradiated and irradiated samples.

over silver irradiated at 20 K. From 30 K onwards individual proton irradiation shows the greater enhancement of $I_c^{\min}$.

Fig. 3 shows the 20 K angle dependence of four samples at a range of magnetic field, 1 T–8 T. At lower magnetic field of 1 T, silver irradiated sample and combined sample shows more than 40% increased performance over proton irradiated samples. In this work, silver irradiation is done at lower fluence compared to proton irradiation which results in a low density of columnar defects compared to density of point defects. In the low magnetic field regime, a lower density of strong pinning centers is favored which is reflected in Fig. 4 as a better I_c performance for silver irradiated sample in a magnetic field below 4 T. As magnetic field increases, 5 T and above, a high density of pinning centers is favored which results in a higher performance of the combined irradiated sample which has a greater number of flux pinning centers than individual irradiation. Silver irradiated sample and combined sample shows more than 40% increased performance over proton irradiated samples. In this work, silver irradiation is done at lower fluence compared to proton irradiation which results in a low density of columnar defects compared to density of point defects. In the low magnetic field regime, a lower density of strong pinning centers is favored which is reflected in Fig. 4 as a better I_c performance for silver irradiated sample in a magnetic field below 4 T. As the magnetic field increases, 5 T and above, a high density of pinning centers is favored which results in a higher performance of the combined irradiated sample which has a greater number of flux pinning centers than individual irradiation.

B. Maximum Entropy Model

The structure-property relationship between defects and critical current can be quantified by fitting the pinning profile using maximum entropy distributions of the vortex path model

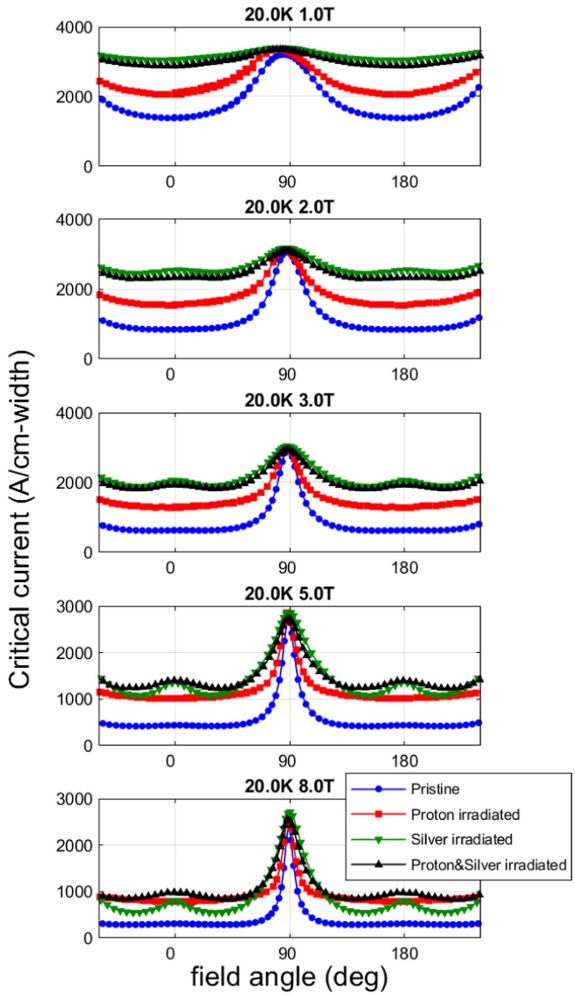

Fig. 3. Angle dependence of the critical current of the sample before irradiation and samples with proton, silver, and combined irradiation at 20 K and magnetic field range of 1 T–8 T.

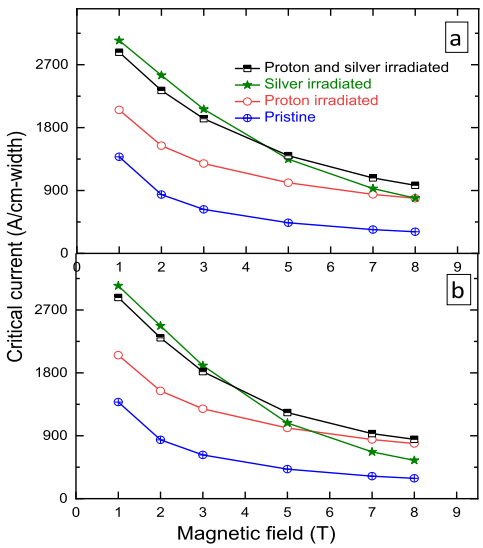

Fig. 4. Field dependences of the critical current at 20 K (a) perpendicular field, and (b) the angular minimum, for the unirradiated and irradiated samples.

TABLE I
PARAMETERS OF FIT COMPONENTS IN FIG. 5

SAMPLES	C-AXIS LORENTZIAN		AB LORENTZIAN		BROAD LORENTZIAN	
	INTENSITY	GAMMA	INTENSITY	GAMMA	INTENSITY	GAMMA
PRISTINE	0	-	464	.08	867	0.9
PROTON	0	-	295	.07	2176	0.9
SILVER	547	0.3	863	0.19	1137	0.9
PROTON&SILVER	761	0.44	512	0.13	1386	0.9

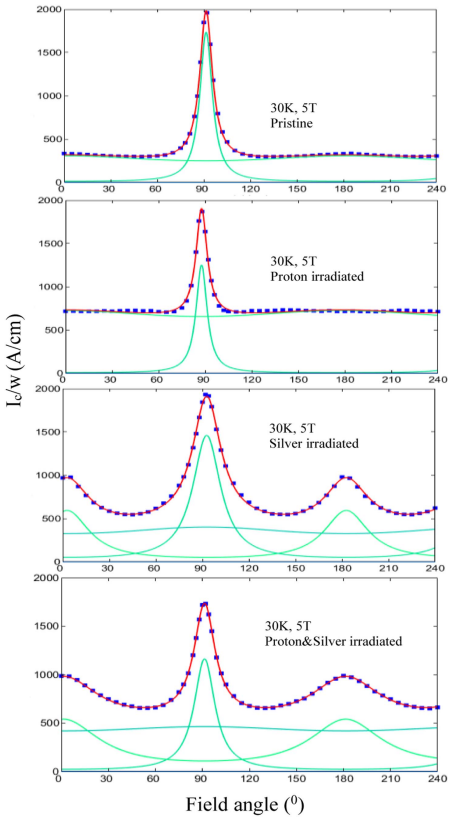

Fig. 5. Decomposition of the angular dependence of I_c into maximum-entropy components at 30 K, 5 T for a) pristine b) sample irradiated with protons c) sample irradiated with silver ions d) sample irradiated with silver and proton ions.

[21], [22] as shown in Fig. 5. Two Lorentzian components (*ab*-Lorentzian, broad *c*-axis Lorentzian) are needed for the fitting of pristine and proton irradiated samples whereas in silver and proton+silver irradiated samples an additional sharper *c*-axis Lorentzian is also required. The peak intensity I_0 and peak width parameter Γ of the fitted components are listed in Table I, where the Lorentzian functional form is as used in [18]. The location of the peak reflects a dominant pinning defect while other defects can contribute to broadening the peak through accommodating staircase vortices [23], [24], [25], [26].

The *ab*-Lorentzian at 30 K represents pinning dominated by intrinsic pinning by the YBCO structure. Interactions with as-grown defects (isotropic pinning centers and *c*-axis pinning centers give some width to this peak in the pristine sample. The addition of more point defects by proton irradiation doesn't change the line shape function (Γ value). However, the addition of *c*-axis columnar defects by silver irradiation results in strengthened interactions between planar pins and columnar defects, accommodating a wider distribution of staircase vortices and resulting in a broadening of the *ab*-Lorentzian peak and a larger Γ. The combination of proton and silver irradiated defects reduces the relative contribution of the *c*-axis defects and thus reduces Γ relative to silver alone. The broad Lorentzian component ($\Gamma \approx 1$) in the pristine sample represents pinning by point defects and nanoparticles already present in the sample which are formed during the growth process as part of the optimization of the conductor for critical current at low temperature and high magnetic field. The addition of extra point defects by proton irradiation results in dramatic increase of this isotropic intensity in proton irradiated sample.

The addition of columnar defects introduces a new Lorentzian with a strong *c*-axis (0°) peak in silver irradiated sample and the combined sample. Addition of protons and silver ions results in a slight broadening of the *c*-axis Lorentzian while sharpening the *ab* Lorentzian relative to silver alone. The almost-isotropic Lorentzian function has a slight *c*-axis bias for the pristine and proton-irradiated samples and a slight *ab*-plane bias for the silver irradiated samples with columnar defects. This is a minor shift that can be regarded as a result of a simplified fitting process where we use 3 components to model a hugely complex real system.

IV. CONCLUSION

Individual proton irradiation and silver irradiation to the optimized fluence results in significant enhanced *c*-axis pinning. The decreased *c*-axis peak enhancement of proton irradiated defects at higher temperature and limited angular range pinning benefit of columnar defects by silver irradiation can be improved by combining the two types of irradiations to the same fluences. The analysis by maximum entropy model gives a comparison of individual irradiation and combined irradiation in terms of available vortex paths and the effective vortex pinning by different types of pinning centers. The overall increase in the *c*-axis I_c at higher magnetic field (5 T–8 T) over a broader angular range gives an overall benefit of combining irradiations relative to irradiations especially at lowest temperatures. At 20 K the combination retains the low-field benefit of columnar defects and the high-field benefit of point defects.

REFERENCES

[1] J. L. MacManus-Driscoll and S. C. Wimbush, "Processing and application of high-temperature superconducting coated conductors," *Nature Rev. Mater.*, vol. 6, 2021, pp. 587–604.
[2] I. A. Sadovskyy et al., "Toward superconducting critical current by design," *Adv. Mater.*, vol. 28, pp. 4593–4600, 2016.

[3] W.-K. Kwok, U. Welp, A. Glatz, A. E. Koshelev, K. J. Kihlstrom, and G. W. Crabtree, "Vortices in high-performance high-temperature superconductors," *Rep. Prog. Phys.*, vol. 79, 2016, Art. no. 116501.
[4] J. L. MacManus-Driscoll et al., "Strongly enhanced current densities in superconducting coated conductors of $YBa_2Cu_3O_{7-x}$ + $BaZrO_3$," *Nat. Mater.*, vol. 3, pp. 439–443, 2004.
[5] J. Gutiérrez et al., "Strong isotropic flux pinning in solution-derived $YBa_2Cu_3O_{7-x}$ nanocomposite superconductor films," *Nat. Mater.*, vol. 6, pp. 367–373, 2007.
[6] L. Civale et al., "Defect independence of the irreversibility line in proton-irradiated Y-Ba-Cu-O crystals," *Phys. Rev. Lett.*, vol. 65, no. 9, pp. 1164–1167, 1990.
[7] Y. Jia et al., "Doubling the critical current density of high temperature superconducting coated conductors through proton irradiation," *Appl. Phys. Lett.*, vol. 103, no. 12, Sep. 2013, Art. no. 122601.
[8] P. L. Civale et al., "Vortex confinement by columnar defects in $YBa_2Cu_3O_7$ crystals: Enhanced pinning at high fields and temperatures," *Phys. Rev. Lett.*, vol. 67, no. 5, pp. 648–651, Jul. 1991.
[9] T. Sueyoshi, "Modification of critical current density anisotropy in high-T_c superconductors by using heavy-ion irradiations," *Quantum Beam Sci.*, vol. 5, 2021, Art. no. 16.
[10] N. M. Strickland et al., "Flux pinning by discontinuous columnar defects in 74 MeV Ag-irradiated $YBa_2Cu_3O_7$ coated conductors," *Physica C: Supercond.*, vol. 469, no. 23, pp. 2060–2067, Dec. 2009.
[11] N. M. Strickland et al., "Isotropic and anisotropic flux pinning induced by heavy-ion irradiation," *IEEE Trans. Appl. Supercond.*, vol. 32, no. 4, Jun. 2022, Art no. 8000505.
[12] N. M. Strickland et al., "Near-isotropic enhancement of the 20 K critical current of $REBa_2Cu_3O_7$ coated conductors from columnar defects," *Supercond. Sci. Technol.*, 2023, doi: 10.1088/1361-6668/acbac6.
[13] M. W. Rupich et al., "Second generation wire development at AMSC," *IEEE Trans. Appl. Supercond.*, vol. 23, no. 3, Jun. 2013, Art. no. 6601205.
[14] Y. Zhang, M. W. Rupich, V. Solovyov, Q. Li, and A. Goyal, "Dynamic behavior of reversible oxygen migration in irradiated-annealed high temperature superconducting wires," *Sci. Rep.*, vol. 10, no. 1, 2020, Art. no. 14848, doi: 10.1038/s41598-020-70663-1.
[15] N. M. Strickland et al., "Effect of annealing high-dose heavy-ion irradiated high-temperature superconductor wires," *Nucl. Instruments Methods Phys. Res., Sect. B: Beam Interact. with Mater. At.*, vol. 409, 2017, pp. 351–355, doi: 10.1016/j.nimb.2017.01.015.
[16] N. M. Strickland, C. Hoffmann, and S. C. Wimbush, "A 1 kA-class cryogen-free critical current characterization system for superconducting coated conductors," *Rev. Sci. Instrum.*, vol. 85, 2014, Art. no. 113907.
[17] N. M. Strickland et al., "Extended-performance supercurrent cryogen-free transport critical-current measurement system," *IEEE Trans. Appl. Supercond.*, vol. 31, no. 5, Aug. 2021, Art. no. 9000305.
[18] N. M. Strickland, A. A. Soman, M. W. Rupich, and S. C. Wimbush, "Onset temperature of intrinsic pinning in a REBCO coated conductor from critical current anisotropy," *Superconductivity*, vol. 4, 2022, Art. no. 100025.
[19] M. Toulemonde, S. Bouffard, and F. Studer, "Swift heavy ions in insulating and conducting oxides: Tracks and physical properties," *Nucl. Instrum. Meth. B*, vol. 91, pp. 108–123, 1994.
[20] A. A. Soman et al., 2023, to be published.
[21] N. J. Long et al., "Relating critical currents to defect populations in superconductors," *IEEE Trans. Appl. Supercond.*, vol. 23, no. 3, Jun. 2013, Art. no. 8001705.
[22] A. A. Soman et al., "The role of stacking faults in the enhancement of the *a-b* plane peak in silver ion-irradiated commercial MOD REBCO wires," *IEEE Trans. Appl. Supercond.*, vol. 32, no. 4, Jun. 2022, Art. no. 8000405.
[23] E. Seiler, F. Gömöry, R. Ries, and M. Vojenčiak, "Analysis of critical current anisotropy in commercial coated conductors in terms of the maximum entropy approach," *Supercond. Sci. Technol.*, vol. 32, no. 9, 2019, Art. no. 095004, doi: 10.1088/1361-6668/ab24ad.
[24] N. J. Long, N. M. Strickland, and E. F. Talantsev, "Modeling of vortex paths in HTS," *IEEE Trans. Appl. Supercond.*, vol. 17, no. 2, pp. 3684–3687, Jun. 2007.
[25] N. J. Long, "Model for the angular dependence of critical currents in technical superconductors," *Supercond. Sci. Technol.*, vol. 21, no. 2, Jan. 2008, Art. no. 025007.
[26] N. J. Long, "Critical current anisotropy in relation to the pinning landscape," in *Vortices and Nanostructured Superconductors*, A. Crisan, Ed. Cham, Switzerland: Springer, 2008, doi: 10.1007/978-3-319-59355-5_4.